HHS Public Access

Author manuscript

Nat Commun. Author manuscript; available in PMC 2015 November 27.

Published in final edited form as:

Nat Commun. ; 6: 7174. doi:10.1038/ncomms8174.

Activating MET Kinase Rearrangements in Melanoma and Spitz Tumors

Iwei Yeh[1,2,*], **Thomas Botton**[1,2], **Eric Talevich**[1,2], **A. Hunter Shain**[1,2], **Alyssa J. Sparatta**[1,2], **Arnaud de la Fouchardiere**[3], **Thaddeus W. Mully**[1], **Jeffrey P. North**[1], **Maria C. Garrido**[1,2], **Alexander Gagnon**[1], **Swapna S. Vemula**[1], **Timothy H. McCalmont**[1,2], **Philip E. LeBoit**[1,2], and **Boris C. Bastian**[1,2,*]

[1] Departments of Dermatology and Pathology, and Helen Diller Family Comprehensive Cancer Center, University of California San Francisco, San Francisco, CA.

[2] Helen Diller Family Comprehensive Cancer Center, University of California San Francisco, San Francisco, CA.

[3] Département de Biopathologie, Centre Léon Bérard, Lyon, France

Abstract

Oncogenic gene fusions have been identified in many cancers and many serve as biomarkers or targets for therapy. Here we identify six different melanocytic tumors with genomic rearrangements of *MET* fusing the kinase domain of MET in-frame to six different N-terminal partners. These tumors lack activating mutations in other established melanoma oncogenes. We functionally characterize two of the identified fusion proteins (TRIM4-MET and ZKSCAN1-MET) and find that they constitutively activate the mitogen-activated protein kinase (MAPK), phosphoinositol-3 kinase (PI3K), and phospholipase C gamma 1 (PLCγ1) pathways. The MET inhibitors cabozantinib (FDA-approved for progressive medullary thyroid cancer) and PF-04217903 block their activity at nanomolar concentrations. MET fusion kinases thus provide a potential therapeutic target for a rare subset of melanoma for which currently no targeted therapeutic options currently exist.

[*]**Corresponding Author Information:** Iwei Yeh, MD, PhD and Boris C. Bastian, MD Departments of Dermatology and Pathology, University of California, San Francisco iwei.yeh@ucsf.edu, boris.bastian@ucsf.edu.

Author Contributions:

Project planning and experimental design: I. Y., T. B., B.C.B.; sample collection: P.E.L., T.H.M., A.F.; histopathologic classification of cohort: I.Y., P.E.L., T.H.M., T.W.M., J.P.N.; preparation of DNA and cDNA libraries: A.G., M.C.G.; aCGH: S.S.V.; sequence data analysis: I.Y., E.W.T., A.H.S.; review of histology and immunohistochemistry: I.Y., A.F.; generation of the translocation constructs: I.Y., A.J.S.; expression vector generation: A.J.S.; *in vitro* experiments including viral transfections and western blotting: A.J.S., T.B.; *in vivo* experiments: A.J.S., T.B.; manuscript writing: I.Y., B.C.B.; review of final manuscript: all authors.

Competing financial interests:

The authors declare no competing financial interests.

Accession codes

The RNA and DNA sequence data have been deposited in the GenBank sequence read archive (SRA) under the accession code SRP033273. The aCGH data have been deposited in the Gene Expression Omnibus database under accession code GSE67841.

Introduction

Constitutive activation of signaling pathways controlling cell growth and proliferation by activating mutations in dominant oncogenes such *BRAF, NRAS, KIT, GNAQ or GNA11* is found in the majority of melanocytic neoplasms[1–5]. These mutations tend to occur early during progression and are found in a mutually exclusive pattern in early stage disease. While inactivating mutations in *NF1* have emerged as an additional genetic alteration[6], a subset of melanomas remains 'wild-type' despite exhaustive studies sequencing the coding regions of genes[7,8]. Recently, we and others described recurrent rearrangements of kinases as a novel class of oncogenic alterations in this subset of melanocytic neoplasms[9–12]. In some cases the resulting breakpoints were affected by copy number changes that increased the gene dosage of the resulting fusion kinases.

In our clinical practice, we perform array comparative genomic hybridization (aCGH) as an adjunct to histopathologic diagnosis for difficult to classify melanocytic tumors. In our database of copy number profiles (n=1202), we noticed cases with copy number transitions within the *MET* locus on chromosome 7q31.2, resulting in amplification or gain of the 3' end of the gene that encodes the kinase domain in 7 of 1202 cases, suggesting the presence of a MET fusion kinase in these cases.

MET is the high-affinity tyrosine kinase receptor for hepatocyte growth factor (HGF). It functions in angiogenesis, cellular motility, growth and invasion[13,14]. In addition, MET plays a role in melanocyte development and homeostasis[15–17]. In 1984, it was identified as a proto-oncogene when TPR-MET, a constitutively active MET fusion kinase, was isolated from a human cell line chemically transformed *in vitro*[18]; however initial reports of TPR-MET expression in human cancer were not replicated[19–21]. *MET* amplification has been observed in various cancers [22–26] and leads to acquired resistance to EGFR inhibitors[27–29]. Recently, alterations within introns of *MET* that alter protein structure have been identified. Splice site mutations that result in exon 14 skipping, deletion within the juxtamembranous domain of MET, and increased MET activity have been identified in lung adenocarcinomas[30,31]. In secondary glioblastomas, fusions within *MET* intron 1 result in the N-terminus of PTPRZ1 fused to the entirety of MET with elevated expression of the MET fusion regulated by the *PTPRZ1* promoter [32].

Here we identify gene rearrangements of MET resulting in in-frame MET kinase fusions in Spitz tumors and melanoma. MET fusions appear in a mutually exclusive pattern with previously identified melanoma oncogenes, are constitutively active and tumorigenic, and thus may serve as therapeutic targets for a subset of melanomas.

Results

Identification of MET kinase fusions

For six of seven cases with copy number transitions within the *MET* locus (those from which leftover archival material was available), we performed targeted sequencing of ~300 melanoma and cancer related genes (Supplementary Data 1-4). Our target regions included *MET* introns 13-16, which we selected as they are situated upstream of the kinase domain

and overlap the areas of copy number transition we identified in *MET*. A rearrangement within intron 14 of *MET* was identified in 4 of the 6 tumors (Fig. 1 and 2, Supplementary Fig. 1 and 2). In the two tumors without detectable *MET* fusions, activating *BRAF* fusions (on chromosome 7q34) were identified instead. The 4 tumors that harbored *MET* fusions demonstrated gain of the distal portion of the long arm of chromosome 7. To look for additional cases with *MET* fusions, we performed targeted sequencing of 41 additional tumors that had copy number gains of the distal portion of the long arm of chromosome 7 (Supplementary Fig. 3, Supplementary Data 5). Most of these tumors had copy number transitions near the *MET* locus but none had copy number transitions within *MET*. However, two of these 41 cases also showed a rearrangement within intron 14 of *MET* by targeted DNA sequencing. None of the 6 cases with *MET* rearrangements had activating mutations in *BRAF*, *NRAS*, *HRAS*, *GNAQ*, *GNA11* or rearrangements of *ALK*, *BRAF*, *NTRK1*, *RET*, *ROS1*.

In five of six cases (all except case 4), an in-frame fusion transcript containing *MET* exons 15-21 was predicted based on the DNA sequence. Out of these five cases, four had tissue available for reverse transcription polymerase chain reaction (RT-PCR), which confirmed the presence of the predicted chimeric transcripts in all cases. In case 4, no 5' partner was identified, as the DNA sequencing data indicated that the 3' portion of *MET* starting from within intron 14 of *MET* was fused to an intergenic region on 7q22.3. Kinome transcriptome sequencing of this case identified in-frame *TRIM4-MET* fusion transcripts joining exon 6 of *TRIM4* to exon 15 of *MET* and we verified this fusion by RT-PCR. Reexamination of the aCGH profile revealed copy number gains with similar amplitudes of the 5' end of *TRIM4*, the intergenic region on 7q22.3 fused to *MET*, and the 3' end of *MET* (Supplementary Fig. 2). Altogether, this indicates a complex rearrangement joining intron 6 of *TRIM4* to a small intergenic region on 7q22.3 and then on to intron 14 of *MET* with subsequent copy number increase of the *MET* fusion kinase.

In case six, two separate breakpoints were identified within *MET* resulting in four detectable fusion junctions between chromosomes 1 and 7 (with only one fusion junction resulting in a predicted in-frame transcript). The aCGH profile demonstrated alternating copy number of the affected portions of chromosomes 1 and 7, raising the possibility that the *MET* fusion was the result of chromothripsis (Supplementary Fig. 4). Thus, in 2 of 6 cases with *MET* fusions, we observed evidence of a complex genomic rearrangement that generated the fusions.

In cases 3 and 5, we observed reciprocal fusion junctions within four hundred base pairs, indicating that the *MET* fusion resulted from a reciprocal translocation event (Fig. 2, Supplementary Fig. 5). In case 3, the copy number profile indicated that reciprocal translocation was followed by a homologous recombination event on the larger derivative chromosome, resulting in loss of heterozygosity of a segment from chromosome 2 and copy number increase of the fusion kinase gene (Fig. 2b,c).

Gain of the *MET* fusion gene was observed in three cases and amplification (log2ratio > 2) was observed in one case (Table 1), suggesting additional selection for increased dosage of the *MET* fusion gene during tumor progression. As expression of the *MET* fusion gene is

driven by the promoter of the 5' partner gene, expression levels should not be related to the basal level of *MET* expression. Additionally, regulation directed at the *MET* promoter should not affect expression of the *MET* fusion. It is expected that the normal expression level of the 5' partner genes in melanocytes determines whether subsequent copy number gain of the *MET* fusion gene constitutes a significant fitness advantage.

In all six cases, the neoplastic melanocytes demonstrated a predominance of fusiform and/or epithelioid morphology with moderate to large amounts of amphophilic cytoplasm. These cytologic features are defining characteristics of Spitz tumors [33]. Four of six cases also demonstrated epidermal hyperplasia and large junctional nests of melanocytes, additional features often seen in Spitz tumors, while Kamino bodies (eosinophilic acellular material at the dermoepidermal junction) and single melanocytes in the upper levels of the epidermis were not observed. We performed MET immunohistochemistry using the three tumors for which material was available. All three cases demonstrated strong diffuse cytoplasmic expression of the kinase domain of MET in neoplastic melanocytes in contrast to common melanocytic nevus control tissue, which showed little or no expression of MET (Fig. 2e, Supplementary Fig. 2d, 4e, 6). While not specific for the MET fusion kinase, these results demonstrate increased expression levels of the kinase domain of MET in tumors with MET fusions compared to common nevi. Immunohistochemistry for p-MET (tyrosine 1234/5) demonstrated increased levels of p-MET compared to conventional melanocytic nevus control tissue (Fig.2, Supplementary Fig. 1, 4, 6).

In all cases, the breakpoint in *MET* occurred within intron 14 upstream of exons 15-21 of *MET*, which encode the entire kinase domain of MET (Fig. 3). Exon 14, which encodes the N-terminal portion of the auto-inhibitory juxtamembrane domain and the Cbl binding site Y1003 (important for ubiquitinization, degradation and downregulation of MET), is notably absent in the *MET* fusions [34]. The diversity of 5' partners of *MET* fusions is similar to the diversity of 5' partners we observed previously for *BRAF* and *ROS1* fusions in Spitz tumors[10,12]. Some of the 5' fusion partners overlap with those previously described: the N-terminus of DCTN1 had been found fused to the kinase domain of ALK and the N-terminus of PPFIBP1 to the kinase domain of ROS1 in Spitz tumors[12]. Similar to the fusion partners of these kinases, the N-terminal fusion partners of MET also contributed multimerization domains, which in five cases were coiled-coil domains and in one case was a SCAN domain (Fig. 3). The finding of an intact MET kinase domain fused to a range of 5' partner genes involved in other oncogenic kinase fusions and/or with multimerization domains suggests that MET fusions are constitutively active.

Functional validation

To assess this directly, we expressed *TRIM4-MET* and *ZKSCAN1-MET* fusion constructs (developed using synthesized theoretical fusion cDNA sequences) in 293FT cells and immortalized mouse melanocytes [35] and found that both fusion kinases were phosphorylated at tyrosine 1234/5 (a marker of kinase activation) under serum-starved conditions with activation of downstream signaling pathways (Fig. 4a, Supplementary Fig, 7). In immortalized mouse melanocytes stably transduced with *TRIM4-MET* or *ZKSCAN1-MET*, no increase in p-MET, p-ERK, p-AKT or p-PLCγ1 was observed after HGF stimulation in

contrast to untransduced melanocytes and melanocytes transduced with wild-type *MET* (Fig. 4a). Insensitivity of the MET fusions to HGF was expected as the extracellular and transmembrane portions of MET are not present and MET fusion kinases are no longer localized to the plasma membrane as supported by cytoplasmic staining by MET and p-MET immunohistochemistry. The absence of wild-type p-MET after HGF stimulation in melanocytes stably expressing MET fusions suggests down-regulation of the endogenous wild-type receptor as a cellular response to constitutive signaling of the fusion kinases. Treatment with 100 nM of cabozantinib (a potent but non-specific MET inhibitor, Food and Drug Administration (FDA) approved for progressive medullary thyroid cancer [36]) or PF-04217903 (a selective MET inhibitor [37]) for 4 hours resulted in decreased p-MET, p-ERK, p-AKT and p-PLCγ1 in melanocytes expressing TRIM4-MET or ZKSCAN1-MET (Fig.4b), demonstrating that both drugs inhibit signaling of MET fusion kinases.

Immortalized mouse melanocytes stably transduced with *ZKSCAN1-MET* formed tumors (n=6 of 6) within 5 weeks of subcutaneous injection into immunocompromised mice, whereas green fluorescent protein (GFP) expressing control cells (n=6) formed no tumors after 12 weeks (Fig. 5), demonstrating that ZKSCAN1-MET is tumorigenic.

Discussion

We identified MET fusion kinases in 0.5% of our cohort of 1202 diagnostically challenging melanocytic tumors by sequencing cases selected for copy number transitions within *MET* (n=6) or copy number gain of the distal portion of the long arm of chromosome 7 (n=41). Our approach likely underestimates the frequency of *MET* fusions in our cohort as such fusions can arise from copy number neutral structural rearrangements.

All cases with *MET* fusions displayed spitzoid histopathologic features and were diagnosed as Spitz tumors or spitzoid melanoma. Spitz tumor refers to a spectrum of tumors, ranging from benign to malignant that includes Spitz nevus (benign), atypical Spitz tumor (ambiguous biologic potential), and spitzoid melanoma (malignant). They are characterized by spindled or epithelioid melanocytes, more commonly arise in children or young adults and have a lower incidence than nevi and melanomas that do not display these cytologic features[33]. Spitz tumors pose unique diagnostic challenges as their histopathologic features are diverse and often overlap with those of *BRAF* and *NRAS* mutant melanoma. Classification of Spitz tumors along the spectrum of benign to malignant shows poor inter-observer reproducibility and poor correlation with clinical outcomes [38]. This may be due to the increased diversity of oncogenic drivers in Spitz tumors as compared to other melanocytic tumors [33]. The tumors with *MET* fusions occurred in young patients (9-29 years old, average 20 years) similar to what we observed in cohorts of melanocytic tumors with other kinase fusions [10,12]. While our cohort of aCGH characterized tumors spans the spectrum of ambiguous melanocytic tumors and includes cases with a possible diagnosis of blue nevus, deep penetrating nevus, ancient nevus, conventional nevus or dysplastic nevus, the majority of cases are Spitz tumors occurring in young patients (Supplementary Table 1). We speculate that *MET* fusions are associated with spitzoid histopathologic features and are more frequent in younger patients, though this remains to be determined. In other solid

tumors such as lung cancer, breast carcinoma, and pancreatic carcinoma, variants enriched for activating kinase fusions occur in younger patients [39–41].

The frequency and age-distribution of activating *MET* fusions in melanoma remains to be determined. Analysis of RNA-seq data from nearly 7700 cancer samples in The Cancer Genome Atlas (TCGA) by Stransky and colleagues identified 6 *MET* fusions in thyroid carcinoma, lung adenocarcinoma, papillary renal carcinoma, low-grade glioma and hepatocellular carcinoma, but not in cutaneous melanoma cases (n=374), indicating that *MET* fusions are rare in cutaneous melanoma[42]. In two of the 6 MET fusions in the TCGA, the MET portion of the fusion transcript began with exon 15, similar to the fusions we identified in melanocytic neoplasms. We did not observe copy number transitions resulting in relative gain of the 3' end of *MET* in the TCGA melanoma cases analyzed by Stransky et al. (aCGH data available for 373 cases). Notably, the median age of TCGA melanoma patients analyzed in this cohort was 56 years with only one patient less than 18 years old (clinical data available for 362 cases).

Our finding of *MET* fusions in tumors that ranged in classification from likely benign to unequivocally malignant indicates that MET fusion kinases occur early during progression. While *MET* fusions appear rare in melanoma, they lead to constitutively active kinases that can be inhibited by approved drugs. As they occur in a mutually exclusive pattern with activating mutations in known melanoma oncogenes they are likely to represent a therapeutic target in a small subset of melanomas.

Methods

Study Population

We analyzed a database of 1202 melanocytic neoplasms, for which array comparative genomic hybridization (aCGH) was performed as part of the diagnostic assessment at the Dermatopathology Section of the Departments of Dermatology and Pathology at the University of California, San Francisco over a thirty-six month period from 2010 through 2013. The majority of these cases are borderline lesions with histopathological features that overlap those of benign nevus and melanoma, for which aCGH was performed as an ancillary diagnostic test. The final diagnosis was determined by review of the final pathology report for each patient. The morphologic classification of the tumor types into Spitz, conventional, deep penetrating nevus-like, or blue was determined by review of the final pathology reports and the microscopic descriptions. The study was approved by the Committee on Human Research and was conducted according to the Declaration of Helsinki. Human tissues were obtained with informed consent during the course of clinical care and a waiver of consent was granted for use of archival material in this study.

DNA and RNA extraction

Areas of tumor were microdissected from 20 μm sections of formalin-fixed, paraffin-embedded (FFPE) tumor. After deparaffinization by washing with Safeclear and ethanol DNA was extracted by phenol chloroform extraction. RNA was extracted from FFPE tumor

after microdissection using the Qiagen RNEasy FFPE kit (p/n 73504) following the manufacturer's protocol.

Array comparative genomic hybridization

aCGH was carried out with 500-1000 ng of genomic DNA on Agilent 4x180k microarrays (Agilent, Santa Clara, CA). The raw microarray images were processed with Agilent Feature Extraction software, and analyzed using Nexus Copy Number Software version 7.0 (Biodiscovery, El Segundo, CA). Cases demonstrating copy number transitions with copy number increase of the 3' portion of *MET* and with sufficient residual DNA or tissue were selected for sequencing. A total of 74 cases were identified with gain of the distal portion of the long arm of chromosome 7 (including the 6 cases with *MET* copy number transitions). Of the 68 cases without copy number transitions in *MET*, 41 with sufficient residual DNA or tissue were selected for sequencing.

DNA sequencing and analysis

Multiplex library preparation was performed using the Ovation Ultralow Library System (NuGEN, San Carlos, CA, p/n 0331-32) or Nextflex (Bioo Scientific, Austin, TX, p/n No. 5140-53) according to the manufacturer's specifications with 200 ng of sample DNA. Hybridization-capture of pooled libraries was performed using custom-designed bait libraries (Nimblegen SeqCap EZ Choice, p/n 06588786001) spanning ~1.8 Mb of the genome including the exons of *BRAF*, *NRAS*, *HRAS*, *KIT*, *GNAQ* and introns 13-16 of *MET* (Supplementary Data 1). The target intervals cover mostly exonic but also some intronic and untranslated regions of 293 (version 1) or 365 target genes (version 2). The target genes were curated to comprise common cancer genes with particular relevance to melanoma.

Captured libraries were sequenced as paired-end 100bp reads on a HiSeq-2000 or HiSeq2500 instrument (Illumina). Sequence reads were mapped to the reference human genome (hg19) using the Burrows-Wheeler aligner (BWA)[43]. Recalibration of reads and variant calling were performed using the Genome Analysis Toolkit (GATK)[44]. Coverage and sequencing statistics were determined using Picard CalculateHsMetrics and Picard CollectInsertSizeMetrics. Variant annotation was performed with Annovar[45]. For fusion detection, read pairs with one or more reads unaligned, insert sizes greater than 1000 bp, or with soft clipping of at least one read were extracted and re-aligned using BWA-SW[46] and used as input to CREST[47]. Structural variants predicted by CREST were reviewed by visual inspection in the Integrative Genomics Viewer[48]. We predicted the resulting fusion transcripts by joining the exon directly upstream from the genomic breakpoint with the exon directly downstream. Predicted protein sequences were then determined from the predicted transcripts.

RNA sequencing and analysis

Double stranded cDNA was synthesized with the NEBNext mRNA Library Prep Reagent Set for Illumina (New England Biolabs E6100S) with 250 ng of input total RNA. Hybrid selection of indexed, adaptor-ligated libraries was performed using the cDNA Kinome hybridization kit with 612 transcripts of kinases and kinase-related genes (Agilent SureSelect Human Kinome Kit, 5190-4801). Sequencing was performed on the HiSeq-2500

instrument (Illumina) with paired-end 100bp reads. Sequence reads were mapped to the reference human genome (hg19) using Spliced Transcripts Alignment to a Reference (STAR).[49]

Confirmation by RT-PCR

Total RNA extracted from FFPE tissue sections was reverse transcribed with random hexamer primers using the NEBNext RNA First Strand Synthesis module. PCR to detect the fusion identified by genomic sequencing was performed with negative controls (Supplementary Table 2). The transcript fusion sequence was confirmed by Sanger sequencing (Quintara Biosciences).

Plasmid construction

The cDNA of the ZKSCAN1-MET fusion was directly synthesized (GENEWIZ, Inc) and subsequently cloned into pENTR with the DTOPO cloning kit as per manufacturers instructions. Subsequently, the cDNA was cloned by LR Clonase II (Life Technologies) into the pLenti6.3/TO/V5-Dest backbone (Life Technologies).

Generation of Stably Transduced Cell lines

Melan-a cells were generously provided by Dr. Dorothy C. Bennett (St. George's Hospital, University of London, London, UK)[50] and maintained in glutamine-containing RPMI-1640 supplemented with 10% heat-inactivated fetal bovine serum, 200 nM of 12-O-tetradecanoylphorbol-13-acetate (TPA), penicillin (100 units/mL) and streptomycin (50 mg/mL). 293FT cells were purchased from Life Technologies and maintained in DME-H21 medium containing 10% heat inactivated fetal bovine serum, minimal essential media (MEM) Non-Essential Amino Acids (0.1 mM), sodium pyruvate (1 mM), penicillin (100 units/mL) and streptomycin (50 mg/mL).

Lentiviruses were produced by transfecting 293FT cells with plasmid DNA (pLenti6.2-GFP or pLenti6.3/TO/V5-Dest-ZKSCAN1-MET with pCMV-VSV-G and pCMV delta R8.2 using Lipofectamine 2000 (Life Technologies). Stably transduced melan-a cells expressing ZKSCAN1-MET were generated by infection with lentivirus in the presence of 10μg/ml of polybrene (Santa Cruz Biotechnology). Cells were selected for at least 20 days using 5 μg/ml of blasticidin S-hydrochloride (Life Technologies) after lentiviral infection.

Drug studies

The FDA-approved MET inhibitor cabozantinib[51] and more selective MET inhibitor PF04217903[37] were purchased from Selleckchem (Houston, TX). Stably transduced melan-a cells were treated with glutamine-containing RPMI-1640 with and without drug (100 nM) for four hours before collection of lysates.

Western Blotting

Antibodies: anti-phospho-Erk (#9101), anti-Met (#8198), anti-phospho-Met (Tyr1234/1235) (#3077), anti-phospho-PLCγ1 (Tyr783) (#2821), from Cell Signaling Technologies, anti-HSP60 (sc-1722) from Santa Cruz Biotechnology. Cell lysates were prepared in RIPA buffer supplemented with Halt protease and phosphatase inhibitor cocktail (Thermo

Scientific). Equal amounts of protein, as measured by bicinchoninic (BCA) protein assay, were resolved in 4-12% Bis-Tris NuPage gradient gels (Life Technologies) and transferred electrophoretically to a polyvinylidene difluoride 0.45 μM membrane. Membranes were blocked in 5% non-fat milk in Tris-buffered saline and Tween 20 (TBST) before being incubated overnight at 4° C with the primary antibodies (1:1000 dilution in 5% non-fat milk in TBST). Signal detection was achieved by incubation of the membrane in enhanced chemiluminiscent (ECL) solution (Millipore) and autoradiography film exposure. The full blots are shown in Supplementary Figs. 8 and 9.

Tumorigenicity study

Animal experiments were carried out in accordance with the Declaration of Helsinki and were approved by the ethical committee of the University of California, San Francisco. Bilateral injections of 1.5 million melan-a cells stably transduced with the *ZKSCAN1-MET* fusion or a *GFP* control vector were performed on 6-week-old female non-obese diabetic/severe combined immunodeficiency, interleukin-2-Rγ^{null} mice. Detection of tumor was performed by palpation 3 times a week and tumor volumes were calculated using the formula $V=(L \times W^2)/2$ over a period of 12 weeks or until the animal had to be euthanized.

Supplementary Material

Refer to Web version on PubMed Central for supplementary material.

Acknowledgments

This work was funded by grants from the National Institutes of Health P01 CA025874 (to B.C.B, I.Y. and T. B.), the Dermatology Foundation (to I. Y.) and the Melanoma Research Alliance (to I. Y.) and the Melanoma Research Foundation (to I. Y.). We thank Sonia Mirza and Jingly Weier for assistance with DNA extraction and aCGH and Arthur Delance for assistance with DNA and cDNA sequencing library preparation.

References

1. Davies H, et al. Mutations of the BRAF gene in human cancer. Nature. 2002; 417:949–954. [PubMed: 12068308]
2. Pollock PM, et al. High frequency of BRAF mutations in nevi. Nat Genet. 2003; 33:19–20. [PubMed: 12447372]
3. Curtin JA, Busam K, Pinkel D, Bastian BC. Somatic activation of KIT in distinct subtypes of melanoma. J. Clin. Oncol. Off. J. Am. Soc. Clin. Oncol. 2006; 24:4340–4346.
4. Van Raamsdonk CD, et al. Frequent somatic mutations of GNAQ in uveal melanoma and blue naevi. Nature. 2009; 457:599–602. [PubMed: 19078957]
5. Van Raamsdonk CD, et al. Mutations in GNA11 in Uveal Melanoma. N. Engl. J. Med. 2010; 363:2191–2199. [PubMed: 21083380]
6. Nissan MH, et al. Loss of NF1 in cutaneous melanoma is associated with RAS activation and MEK dependence. Cancer Res. 2014 doi:10.1158/0008- 5472.CAN-13-2625.
7. Krauthammer M, et al. Exome sequencing identifies recurrent somatic RAC1 mutations in melanoma. Nat. Genet. 2012; 44:1006–1014. [PubMed: 22842228]
8. Hodis E, et al. A landscape of driver mutations in melanoma. Cell. 2012; 150:251–263. [PubMed: 22817889]
9. Palanisamy N, et al. Rearrangements of the RAF kinase pathway in prostate cancer, gastric cancer and melanoma. Nat. Med. 2010; 16:793–798. [PubMed: 20526349]

10. Botton T, et al. Recurrent BRAF kinase fusions in melanocytic tumors offer an opportunity for targeted therapy. Pigment Cell Melanoma Res. 2013:n/a–n/a. doi:10.1111/pcmr.12148.
11. Hutchinson KE, et al. BRAF fusions define a distinct molecular subset of melanomas with potential sensitivity to MEK inhibition. Clin. Cancer Res. Off. J. Am. Assoc. Cancer Res. 2013; 19:6696–6702.
12. Wiesner T, et al. Kinase fusions are frequent in Spitz tumours and spitzoid melanomas. Nat. Commun. 2014; 5
13. Bottaro DP, et al. Identification of the hepatocyte growth factor receptor as the c-met proto-oncogene product. Science. 1991; 251:802–804. [PubMed: 1846706]
14. Stoker M, Gherardi E, Perryman M, Gray J. Scatter factor is a fibroblastderived modulator of epithelial cell mobility. Nature. 1987; 327:239–242. [PubMed: 2952888]
15. Kos L, et al. Hepatocyte growth factor/scatter factor-MET signaling in neural crest-derived melanocyte development. Pigment Cell Res. Spons. Eur. Soc. Pigment Cell Res. Int. Pigment Cell Soc. 1999; 12:13–21.
16. McGill GG, Haq R, Nishimura EK, Fisher DE. c-Met expression is regulated by Mitf in the melanocyte lineage. J. Biol. Chem. 2006; 281:10365–10373. [PubMed: 16455654]
17. Beuret L, et al. Up-regulation of MET Expression by {alpha}-Melanocytestimulating Hormone and MITF Allows Hepatocyte Growth Factor to Protect Melanocytes and Melanoma Cells from Apoptosis. J Biol Chem. 2007; 282:14140–14147. [PubMed: 17371876]
18. Cooper CS, et al. Molecular cloning of a new transforming gene from a chemically transformed human cell line. Nature. 1984; 311:29–33. [PubMed: 6590967]
19. Soman NR, Correa P, Ruiz BA, Wogan GN. The TPR-MET oncogenic rearrangement is present and expressed in human gastric carcinoma and precursor lesions. Proc. Natl. Acad. Sci. 1991; 88:4892–4896. [PubMed: 2052572]
20. Osaki M, et al. Lack of rearranged Tpr-met mRNA expression in human gastric cancer cell lines and gastric mucosa and carcinoma. Anticancer Res. 1996; 16:2881–2884. [PubMed: 8917402]
21. Heideman DAM, et al. Absence of tpr–met and expression of c-met in human gastric mucosa and carcinoma. J. Pathol. 2001; 194:428–435. [PubMed: 11523050]
22. Kuniyasu H, et al. Frequent amplification of the c-met gene in scirrhous type stomach cancer. Biochem. Biophys. Res. Commun. 1992; 189:227–232. [PubMed: 1333188]
23. Di Renzo MF, et al. Overexpression and amplification of the met/HGF receptor gene during the progression of colorectal cancer. Clin. Cancer Res. Off. J. Am. Assoc. Cancer Res. 1995; 1:147–154.
24. Fischer U, et al. Amplification of the MET gene in glioma. Genes. Chromosomes Cancer. 1995; 12:63–65. [PubMed: 7534113]
25. Beau-Faller M, et al. MET gene copy number in non-small cell lung cancer: molecular analysis in a targeted tyrosine kinase inhibitor naïve cohort. J. Thorac. Oncol. Off. Publ. Int. Assoc. Study Lung Cancer. 2008; 3:331–339.
26. Yamamoto S, et al. Gene amplification and protein overexpression of MET are common events in ovarian clear-cell adenocarcinoma: their roles in tumor progression and prognostication of the patient. Mod. Pathol. Off. J. U. S. Can. Acad. Pathol. Inc. 2011; 24:1146–1155.
27. Bean J, et al. MET amplification occurs with or without T790M mutations in EGFR mutant lung tumors with acquired resistance to gefitinib or erlotinib. Proc. Natl. Acad. Sci. U. S. A. 2007; 104:20932–20937. [PubMed: 18093943]
28. Engelman JA, et al. MET amplification leads to gefitinib resistance in lung cancer by activating ERBB3 signaling. Science. 2007; 316:1039–1043. [PubMed: 17463250]
29. Bardelli A, et al. Amplification of the MET receptor drives resistance to anti- EGFR therapies in colorectal cancer. Cancer Discov. 2013; 3:658–673. [PubMed: 23729478]
30. Kong-Beltran M, et al. Somatic mutations lead to an oncogenic deletion of met in lung cancer. Cancer Res. 2006; 66:283–289. [PubMed: 16397241]
31. Cancer Genome Atlas Research Network. Comprehensive molecular profiling of lung adenocarcinoma. Nature. 2014; 511:543–550. [PubMed: 25079552]

32. Bao Z-S, et al. RNA-seq of 272 gliomas revealed a novel, recurrent PTPRZ1-MET fusion transcript in secondary glioblastomas. Genome Res. 2014:gr.165126.113. doi:10.1101/gr.165126.113.
33. Bastian BC. The Molecular Pathology of Melanoma: An Integrated Taxonomy of Melanocytic Neoplasia. Annu. Rev. Pathol. Mech. Dis. 2014; 9:239–271.
34. Peschard P, et al. Mutation of the c-Cbl TKB domain binding site on the Met receptor tyrosine kinase converts it into a transforming protein. Mol. Cell. 2001; 8:995–1004. [PubMed: 11741535]
35. Bennett DC, Cooper PJ, Hart IR. A line of non-tumorigenic mouse melanocytes, syngeneic with the B16 melanoma and requiring a tumour promoter for growth. Int. J. Cancer. 1987; 39:414–418. [PubMed: 3102392]
36. Elisei R, et al. Cabozantinib in progressive medullary thyroid cancer. J. Clin. Oncol. Off. J. Am. Soc. Clin. Oncol. 2013; 31:3639–3646.
37. Cui JJ, et al. Discovery of a novel class of exquisitely selective mesenchymalepithelial transition factor (c-MET) protein kinase inhibitors and identification of the clinical candidate 2-(4-(1-(quinolin-6-ylmethyl)-1H-[1,2,3]triazolo[4,5- b]pyrazin-6-yl)-1H-pyrazol-1-yl)ethanol (PF-04217903) for the treatment of cancer. J. Med. Chem. 2012; 55:8091–8109. [PubMed: 22924734]
38. Barnhill RL, et al. Atypical Spitz nevi/tumors: lack of consensus for diagnosis, discrimination from melanoma, and prediction of outcome. Hum. Pathol. 1999; 30:513–520. [PubMed: 10333219]
39. Tognon C, et al. Expression of the ETV6-NTRK3 gene fusion as a primary event in human secretory breast carcinoma. Cancer Cell. 2002; 2:367–376. [PubMed: 12450792]
40. Pan Y, et al. ALK, ROS1 and RET fusions in 1139 lung adenocarcinomas: A comprehensive study of common and fusion pattern-specific clinicopathologic, histologic and cytologic features. Lung Cancer. 2014; 84:121–126. [PubMed: 24629636]
41. Chmielecki J, et al. Comprehensive Genomic Profiling of Pancreatic Acinar Cell Carcinomas Identifies Recurrent RAF Fusions and Frequent Inactivation of DNA Repair Genes. Cancer Discov. 2014; 4:1398–1405. [PubMed: 25266736]
42. Stransky N, Cerami E, Schalm S, Kim JL, Lengauer C. The landscape of kinase fusions in cancer. Nat. Commun. 5. 2014
43. Li H, Durbin R. Fast and accurate short read alignment with Burrows- Wheeler transform. Bioinforma. Oxf. Engl. 2009; 25:1754–1760.
44. McKenna A, et al. The Genome Analysis Toolkit: A MapReduce framework for analyzing next-generation DNA sequencing data. Genome Res. 2010; 20:1297–1303. [PubMed: 20644199]
45. Wang K, Li M, Hakonarson H. ANNOVAR: functional annotation of genetic variants from high-throughput sequencing data. Nucleic Acids Res. 2010; 38:e164–e164. [PubMed: 20601685]
46. Li H, Durbin R. Fast and accurate long-read allignment with Burrows-Wheeler transform. Bioinforma. Oxf. Engl. 2010; 26:589–595.
47. Wang J, et al. CREST maps somatic structural variation in cancer genomes with base-pair resolution. Nat. Methods. 2011; 8:652–654. [PubMed: 21666668]
48. Thorvaldsdóttir H, Robinson JT, Mesirov JP. Integrative Genomics Viewer (IGV): high-performance genomics data visualization and exploration. Brief. Bioinform. 2013; 14:178–192. [PubMed: 22517427]
49. Dobin A, et al. STAR: ultrafast universal RNA-seq aligner. Bioinformatics. 2013; 29:15–21. [PubMed: 23104886]
50. Bennett DC, Cooper PJ, Hart IR. A line of non-tumorigenic mouse melanocytes, syngeneic with the B16 melanoma and requiring a tumour promoter for growth. Int. J. Cancer J. Int. Cancer. 1987; 39:414–418.
51. Yakes FM, et al. Cabozantinib (XL184), a Novel MET and VEGFR2 Inhibitor, Simultaneously Suppresses Metastasis, Angiogenesis, and Tumor Growth. Mol. Cancer Ther. 2011; 10:2298–2308. [PubMed: 21926191]

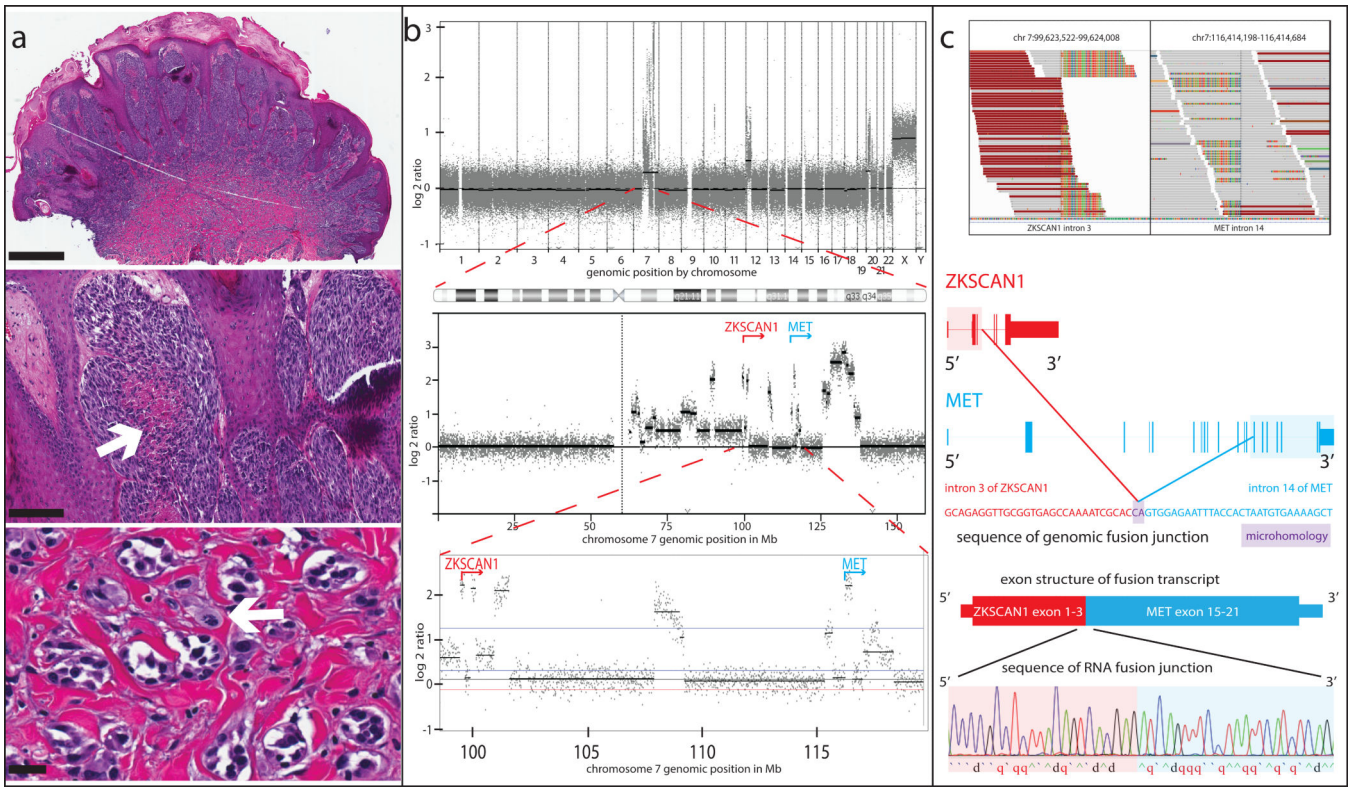

Figure 1. Spitzoid Melanoma with ZKSCAN1-MET fusion

(a) Histopathology (4x, scale bar, 1 mm) showing a dome-shaped nodule with a thickened epidermis and sheets of spindled and epithelioid melanocytes in the dermis, some with central necrosis (20x, arrow, scale bar, 200 μm). High power view (20x, lower panel) demonstrates small nests of melanocytes in infiltrative array and a mitotic figure (arrow) in the deep portion of the tumor. Scale bar, 25 μm. **(b)** aCGH profile (top panel) with copy number increases involving chromosomes 7 and 12p. Chromosome 7 shows amplification of multiple regions on the long arm, including the 5' end of *ZKSCAN1* (red) and the 3' end of *MET* (blue) (lower panels). **(c)** Stacks of sequencing reads from Integrated Genome Viewer spanning the breakpoints, with unaligned portions (rainbow-colored) flanking one side of the fusion junction in *ZKSCAN1* (left) and *MET* (right). Reads whose mate pair maps to the opposite side of the fusion junction are maroon. The DNA sequence of the fusion junction is displayed, with bases that map to *ZKSCAN1* in red, and those that map to *MET* in blue with their corresponding gene models above. Two bases of microhomology at the fusion junction are displayed in purple. The exonic structure of the predicted fusion transcript is shown with the sequencing trace from RT-PCR confirming its expression beneath.

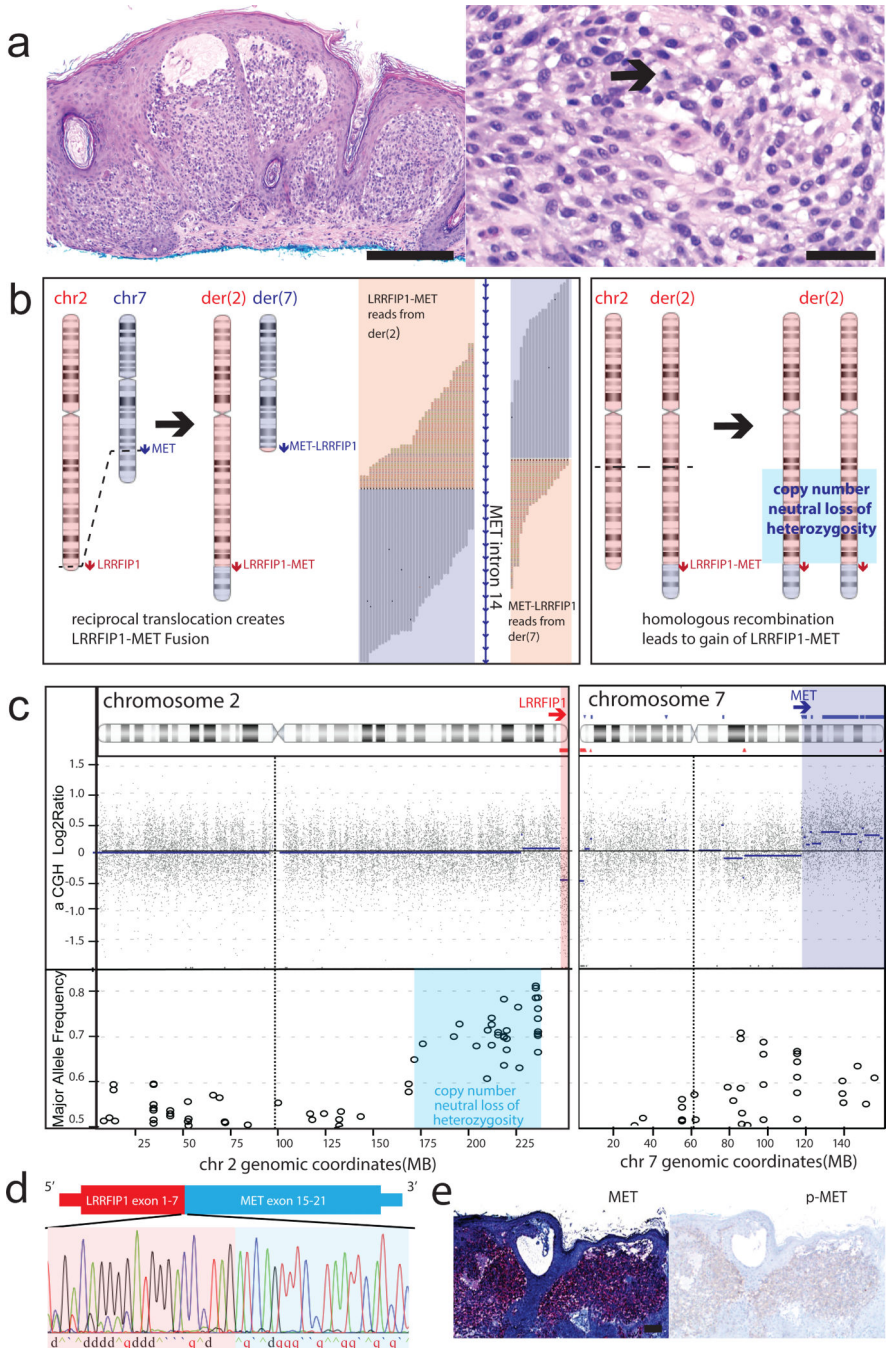

Figure 2. Reciprocal translocation resulting in LRRFIP1-MET fusion in an atypical Spitz tumor

(a) Histopathology showing large nests of epithelioid melanocytes with pericellular clefting (4x, left panel, Scale bar, 300 μm) and scattered mitoses (20x, right panel, arrow, Scale bar, 50 μm) in the papillary dermis under a thickened epidermis. **(b)** Inferred succession of genetic events with supporting genomic data. Left panel: Reciprocal translocation between chromosomes 2 and 7 generates two derivative chromosomes with *LRRFIP1-MET* and *MET-LRRFIP1* fusion genes, respectively. Chimeric reads supporting the fusion junctions are mapped to intron 14 of *MET* with the rainbow colored portion of the reads mapping to

chromosome 2. Right panel: Subsequent homologous recombination of the derivative chromosome 2 results in a region of copy number neutral loss of heterozygosity on 2q and gain of the *LRRFIP1-MET* fusion gene. **(c)** Copy number and major allele frequency plots for chromosomes 2 and 7 demonstrate loss of 2q and gain of 7q distal to the breakpoints and allelic imbalance on 2q. **(d)** The exonic structure of the predicted fusion transcript with the sequencing trace from RT-PCR confirming its expression. **(e)** Strong diffuse expression of the kinase domain of MET is demonstrated by immunohistochemistry, with moderate staining for p-MET (4x, Scale bar, 100 μm).

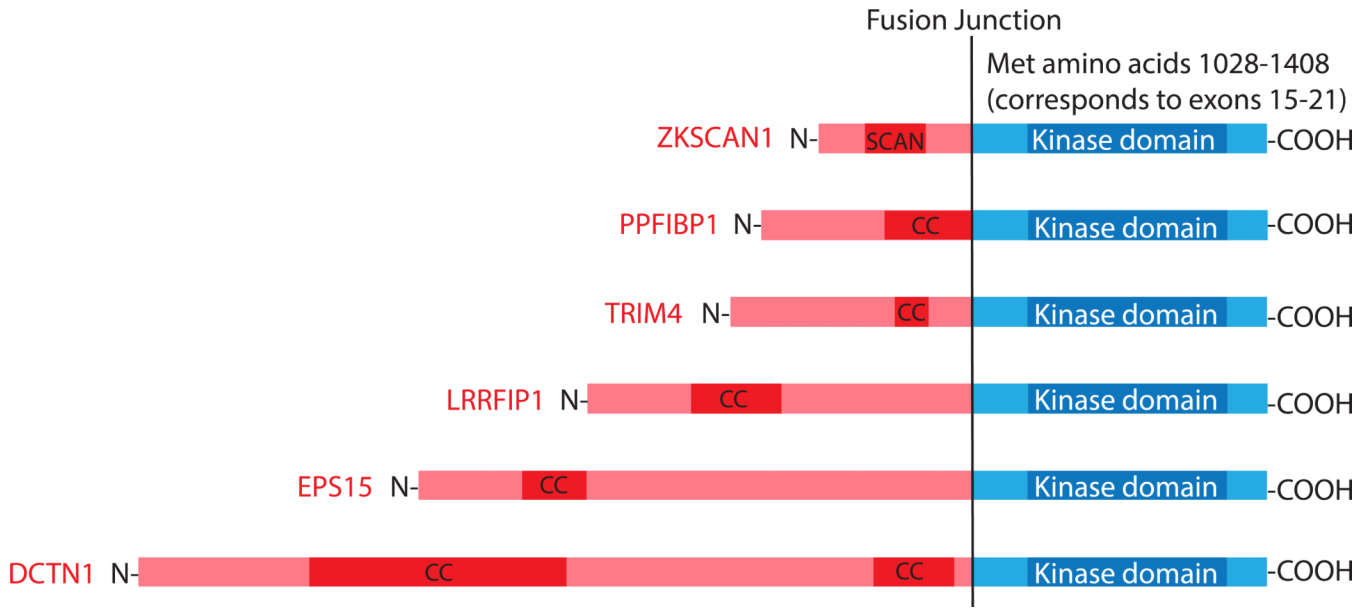

Figure 3. Domain structure of MET Fusions

The portion from the N-terminal partner is displayed in pink with multimerization domains highlighted in red (CC= coiled coil domain, SCAN= SCAN domain). The MET portion (starting from exon 15 in all cases) is colored blue with the kinase domain highlighted in dark blue.

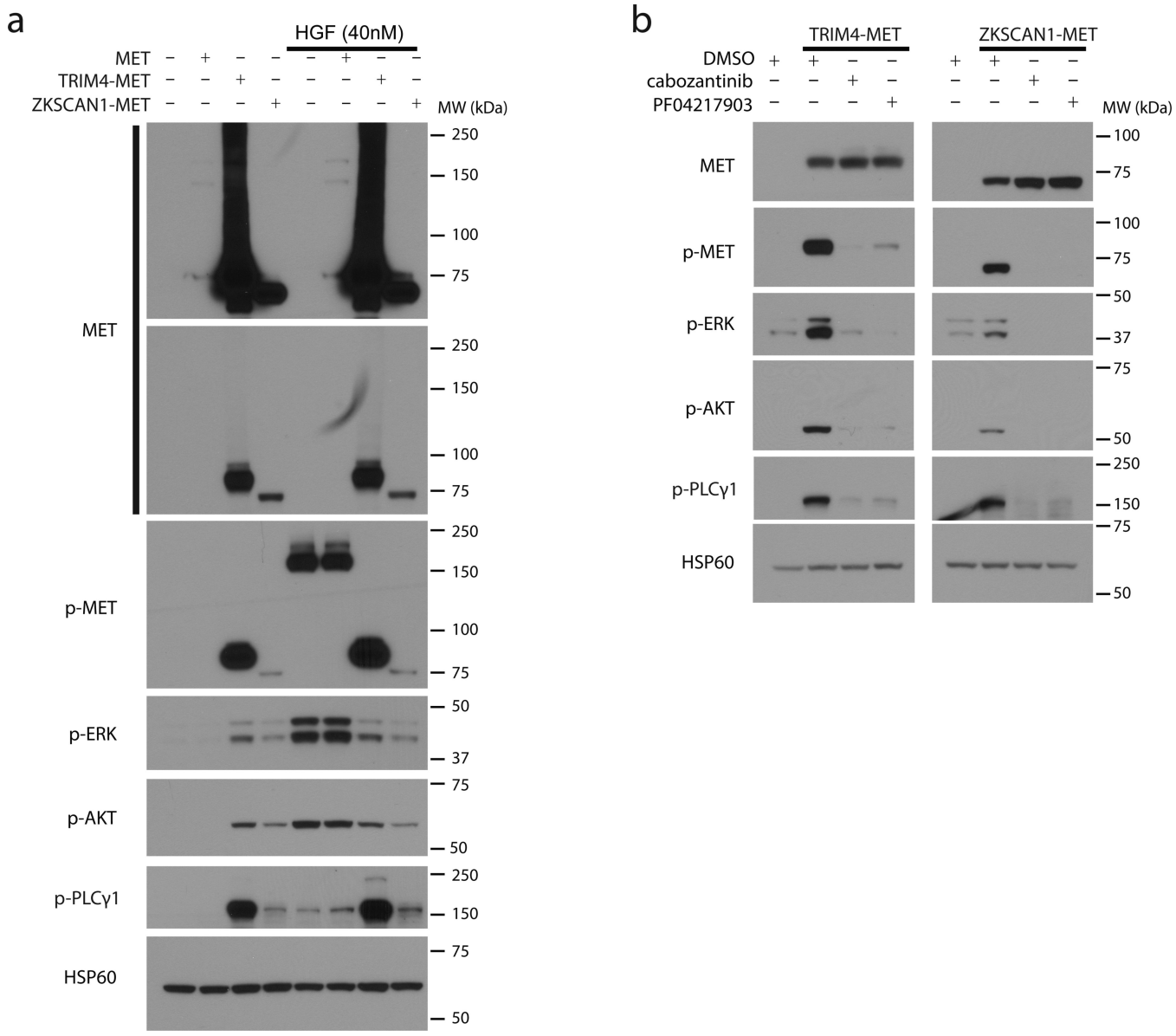

Figure 4. MET fusions constitutively activate oncogenic signaling pathways and are inhibited by cabozantinib and PF-04217903

(a) Melan-a cells (immortalized mouse melanocytes) were stably transduced with full length *MET*, *TRIM4-MET* and *ZKSCAN1-MET* expression constructs. The expressed fusion proteins were detected with by MET antibody at the predicted molecular weights of 79 and 65 kDa (longer exposure upper MET panel, shorter exposure lower MET panel). TRIM4-MET and ZKSCAN1-MET were phosphorylated at tyrosine 1234/1235 in the absence of serum. **(b)** Treatment with cabozantinib or PF-04217903 for four hours (both at 100 nM) significantly decreased p-MET and downstream signaling.

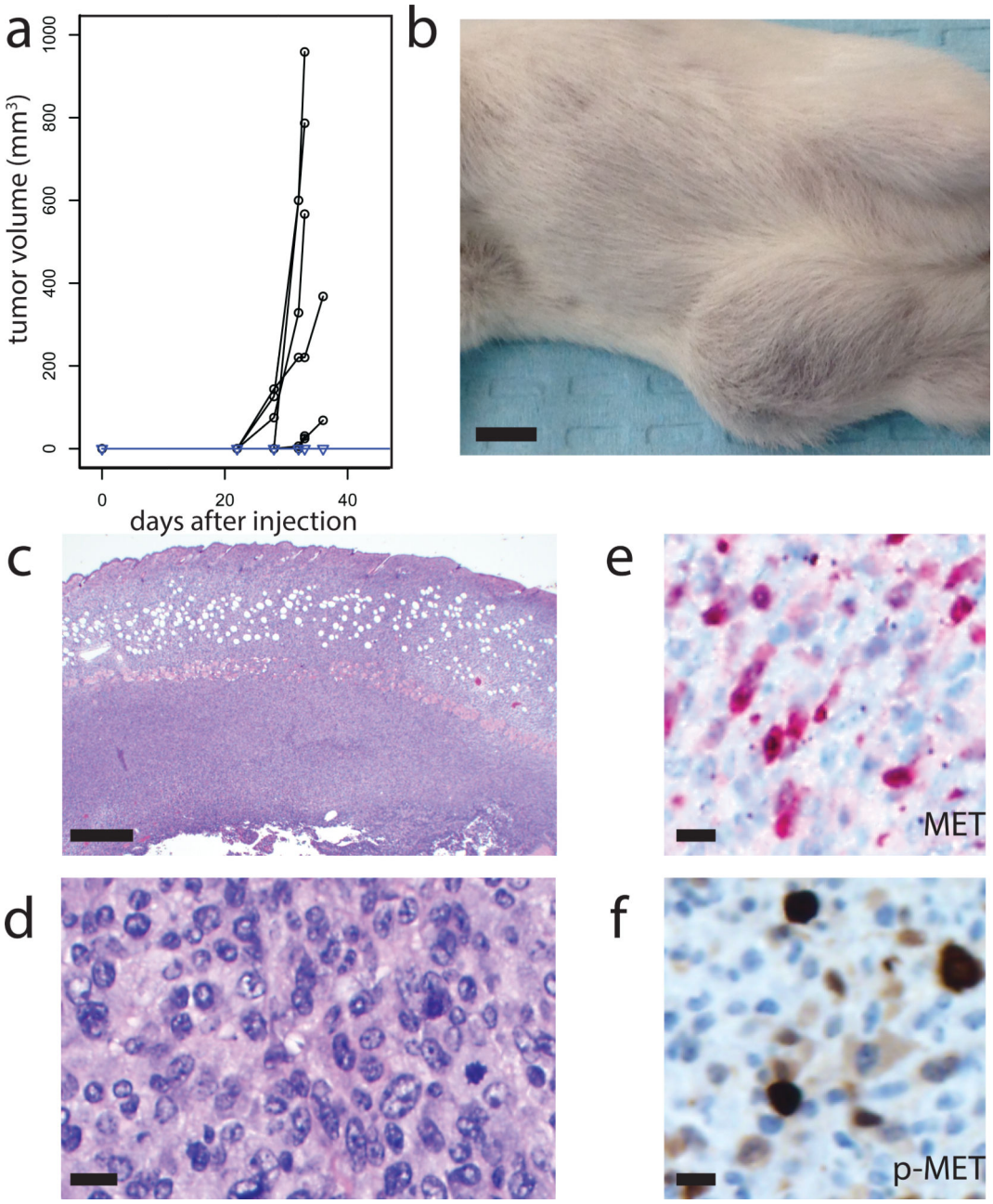

Figure 5. ZKSCAN-1 MET is tumorigenic

(a) Melan-a stably transduced with a *ZKSCAN1-MET* expression construct were injected into NOD/SCID/interleukin 2 receptor γ null mice (1.5 million cells, bilateral flank injections) with matched GFP transduced controls. All six injection sites with ZKSCAN1-MET expressing melan-a cells developed tumors within 5 weeks (black circles), whereas no tumors developed at the sites injected with *GFP* transduced controls (n=6) after 12 weeks (blue triangles). **(b)** Tumor formation 28 days after injection with ZKSCAN1-MET expressing melan-a cells. Scale bar, 0.5 cm. **(c)** Histopathology of ZKSCAN1-MET tumor (4x) demonstrates tumor cells diffusely within the skin and subcutaneous tissue. Scale bar, 500 μm. **(d)** At high power (20x) tumor cells have hyperchromatic and irregularly sized

nuclei and mitoses are present. Scale bar, 10 μm. **(e)** Tumor cells have variable positivity for the kinase domain of MET (20x). Scale bar, 10 μm. **(f)** Tumor cells have variable levels of p-MET positivity (20x). Scale bar, 10 μm.

Table 1

Clinical and genetic features of melanocytic tumors with MET fusion kinase.

Case	Age	Sex	Location	Final diagnosis	Clinical Follow-up	5' Partner	Location of 5' Partner	Copy number transition in MET	Copy number status of 3' end of MET	Expression Confirmed	Rearrangement Type *
1	15	F	thigh	Spitzoid Melanoma	No recurrence (33 months)	*ZKSCAN1*	7q22.1	YES	amp ^	RT-PCR	rearrangement, NOS
2	17	F	foot	Spitzoid Melanoma	NA	*PPFIBP1*	12p11.22	YES	gain	RT-PCR	rearrangement, NOS
3	9	F	cheek	Atypical Spitz Tumor, favor benign	NA	*LRRFIP1*	2q37.3	YES	gain	RT-PCR	reciprocal translocation
4	24	F	buttock	Atypical Spitz Tumor, favor benign	No recurrence (27 months)	*TRIM4*	7q22.1	YES	gain	RNASeq, RT-PCR	complex rearrangement
5	29	F	thigh	Atypical Spitz Tumor	No recurrence after wide local excision (23 months)	*DCTN1*	2p13.1	NO	normal	NA	reciprocal translocation
6	24	F	back	Atypical Spitz Tumor	No recurrence (8 months)	*EPS15*	1p32.3	NO	normal	RT-PCR	complex rearrangement

* Cases in which only the *MET* fusion junction was identified were classified as rearrangement, NOS (not otherwise specified). Cases in which reciprocal fusion junctions were identified were classified as reciprocal translocations. Cases with multiple breakpoints and fusion junctions identified were classified as complex rearrangements.

^ amplification defined as $\log_2$ratio > 2

RNA extracted from FFPE was not sufficient for analysis in this case.